communications psychology

Article

https://doi.org/10.1038/s44271-025-00193-x

Person-centered analyses reveal that developmental adversity at moderate levels and neural threat/safety discrimination are associated with lower anxiety in early adulthood

Check for updates

Lucinda M. Sisk[1] ✉, Taylor J. Keding[1], Sonia Ruiz[1], Paola Odriozola[1], Sahana Kribakaran[1,2], Emily M. Cohodes[1], Sarah McCauley[1], Sadie J. Zacharek[3], Hopewell R. Hodges[4], Jason T. Haberman[1], Jasmyne C. Pierre[5], Camila Caballero[1], Arielle Baskin-Sommers[1,6] & Dylan G. Gee[1,6] ✉

Parsing heterogeneity in the nature of adversity exposure and neurobiological functioning may facilitate better understanding of how adversity shapes individual variation in risk for and resilience against anxiety. One putative mechanism linking adversity exposure with anxiety is disrupted threat and safety learning. Here, we applied a person-centered approach (latent profile analysis) to characterize patterns of adversity exposure at specific developmental stages and threat/safety discrimination in corticolimbic circuitry in 120 young adults. We then compared how the resultant profiles differed in anxiety symptoms. Three latent profiles emerged: (1) a group with lower lifetime adversity, higher neural activation to threat, and lower neural activation to safety; (2) a group with moderate adversity during middle childhood and adolescence, lower neural activation to threat, and higher neural activation to safety; and (3) a group with higher lifetime adversity exposure and minimal neural activation to both threat and safety. Individuals in the second profile had lower anxiety than the other profiles. These findings demonstrate how variability in within-person combinations of adversity exposure and neural threat/safety discrimination can differentially relate to anxiety, and suggest that for some individuals, moderate adversity exposure during middle childhood and adolescence could be associated with processes that foster resilience to future anxiety.

Exposure to adversity during development can shape neural and behavioral maturation, and increases risk for later mental health problems[1,2]. Anxiety disorders have been consistently linked with exposure to adversity during development, and youth who experience one or more adverse exposures are 40% more likely to develop an anxiety disorder by adulthood[3]. Nonetheless, a majority of individuals demonstrate resilience against mental health problems following adversity exposure during development[4]. This heterogeneity in outcomes may reflect—among other psychosocial and systemic factors[5]—variability in both the nature of adversity exposure and in brain and behavioral development[6–9]. In particular, the developmental timing of adversity exposure likely informs its impacts, as maturing neural circuits fluctuate in plasticity across their respective developmental trajectories, potentially rendering both circuits and the cognitive and emotional processes they support differentially sensitive to environmental exposures[8,10–12]. Parsing heterogeneity in features of adversity exposure, such as developmental timing, and variation in neurobehavioral processes may elucidate co-occurring patterns of exposure and functioning that predict risk for and resilience against future mental health problems.

[1]Department of Psychology, Yale University, New Haven, CT, USA. [2]Interdepartmental Neuroscience Program, Yale School of Medicine, New Haven, CT, USA. [3]Department of Brain and Cognitive Sciences, Massachusetts Institute of Technology, Cambridge, MA, USA. [4]Institute of Child Development, University of Minnesota, Minneapolis, MN, USA. [5]Department of Psychology, The City College of New York, New York, NY, USA. [6]These authors contributed equally: Arielle Baskin-Sommers, Dylan G. Gee. ✉e-mail: lucinda.sisk@yale.edu; dylan.gee@yale.edu

Threat and safety learning play a central role in anxiety disorders, and disruptions in these processes and in supporting neural circuitry are evident following adversity exposure during development. Rodent models of threat and safety learning and adversity exposure show that the developmental timing of adversity exposure may differentially shape threat and safety learning and related behavior[13]. For instance, although exposure to adversity during development is generally associated with increased anxiety-like behavior in adulthood in rodent models[14–18], effects of adversity on threat and safety learning vary as a function of age of exposure. Adult female mice exposed to adversity during the neonatal period displayed impaired threat expression[19], while adult mice exposed to adversity during pre-adolescence show delayed discrimination between threat and safety and reduced ability to inhibit fear in the presence of a safety cue[15]. Mice exposed to adversity during adolescence showed altered neuronal firing patterns in the prelimbic cortex in response to threat in adulthood[20]. However, how the developmental timing of adversity exposure affects later functioning may also vary depending on the nature of the stressful exposure. As one example, chronic mild stress during the juvenile and adolescent stages of development may confer greater resilience to future stressors in adulthood[21–26]. While the mechanisms by which such putative resilience might relate to threat and safety learning remain unclear, findings from rodent research highlight the complex interplay between dimensions of adversity, such as developmental timing, and alterations to associative learning processes that may differentially confer greater risk for or resilience against future psychopathology.

Evidence from studies examining threat and safety learning in child, adolescent, and adult human samples suggests that exposure to adversity during development is associated with reduced discrimination between threat and safety cues in aversive learning tasks[27,28]. Lack of discrimination between threat and safety has been observed behaviorally[29], neurally[30], and physiologically[31,32]. Research focusing on threat in particular has identified blunted responses to learned threat cues in individuals exposed to adversity during development[30,32–34]; however, *heightened* responses to threat following adversity exposure during development have also been reported, primarily in studies employing threat stimuli with emotional content[35–37]. Individuals with adversity exposure may also exhibit heightened fear responses to safety cues[38,39], which may be theoretically consistent with an adversity-related reduction in threat/safety discrimination. While few studies have examined the role of developmental timing of adversity in predicting neural response to threat or safety, convergent evidence implicates early childhood and late adolescence as potential sensitive windows during which adversity exposure may shape corticolimbic responses to threatening images through adulthood[40,41]. Clarifying how the timing of adversity exposure might differentially relate to changes in threat/safety discrimination may provide further insight into adversity-related shifts in associative learning and links with future mental health.

The hippocampus, amygdala, dorsal anterior cingulate cortex (dACC), and ventromedial prefrontal cortex (vmPFC) comprise the primary neural regions canonically involved in threat and safety learning[42], as well as in anxiety[43]. Neural responses within regions comprising this circuit—for instance, activation during affective (e.g., threat, reward) learning[44,45] and connectivity during rest[46]—can predict longitudinal emergence of anxiety, and may play an integral role in both short- and long-term threat encoding and extinction[47]. These regions are also among the most sensitive to the effects of exposure to adversity during development[47–49]. Further, regions comprising this corticolimbic circuit are known to develop along different trajectories that mature nonlinearly and reach adult-like states at different times during development[48]. Specifically, the hippocampus and amygdala develop relatively early[49], while prefrontal cortical regions undergo more protracted maturation, demonstrating enhanced neuroplasticity during adolescence[50–53]. Structural connections between these regions are thought to reach maturation later still. For example, the uncinate fasciculus, a white matter tract structurally connecting prefrontal and limbic regions, exhibits ongoing development into adulthood[54]. Given the unique developmental timelines of this circuitry, the ages at which adversity exposure occurs may inform distinct impacts on corticolimbic circuitry and threat and safety learning, contributing to cascading effects on mental health into adulthood[8,55,56]. Further, given developmental shifts in threat and safety learning and responding[27,57–59], parsing how the developmental timing of adversity exposure relates to region-specific neural discrimination between threat and safety in adulthood could provide insight into how adversity exposure may shape both developing neural circuitry and the neural computations it supports. Delineating how co-occurring patterns of adversity and threat/safety discrimination relate to variability in mental health is important for understanding why some individuals––but not others––develop mental health disorders following adversity exposure.

Person-centered approaches may critically aid in parsing heterogeneity across multiple measures by identifying co-occurring patterns that characterize groups of individuals[60–62]. Latent profile analysis (LPA) is one such approach, characterizing 'profiles' of individuals based on shared patterns across a set of continuous variables[63–65]. In the context of threat and safety learning and adversity exposure, LPA facilitates the identification of profiles characterized by *both* brain and adversity measures and may more readily elucidate variation in associations between neural activation and adversity than more widely used univariate approaches. In the present study, we leveraged LPA to identify shared patterns of adversity exposure across development and neural discrimination in corticolimbic regions—specifically, bilateral hippocampus, amygdala, dACC, and regions of the vmPFC—between threat and safety cues during an aversive learning task. Following profile identification, we tested whether the resulting profiles differed in mental health symptoms (i.e., anxiety symptoms, trauma-related symptoms, and externalizing symptoms). We hypothesized that the LPA solution would include a profile characterized by blunted amygdala activation to threat cues, weaker neural discrimination between threat and safety, and greater history of adversity exposure during early childhood[27–32,40]. We further hypothesized that individuals in this profile would display higher levels of anxiety symptoms[3,66]. In addition, we hypothesized that another profile would be characterized by lower levels of adversity exposure across development and stronger discrimination between threat and safety and that individuals in this profile would display lower levels of anxiety. Given that this study is broadly exploratory and presents a novel application of LPA, fitting the model on both adversity exposure at four developmental stages and neural threat and safety discrimination data, we did not have specific hypotheses regarding additional combinations of these variables and anxiety symptoms.

Methods

Participants

Participants were 120 adults between the ages of 18 and 30 recruited from the greater New Haven, CT community as part of an ongoing study on threat and safety learning in the context of anxiety disorders. For detailed demographic information, see Table 1. Participants were right-handed, able to fluently communicate in English, and free from contraindications for MRI scanning (e.g., no braces, metal implants). Additional exclusion criteria included (1) history of concussion or head injury, (2) history of neurological disorder or chronic medical illness, (3) lifetime history of psychotic disorders, conduct disorder, autism spectrum disorder, bipolar disorder, non-alcohol or non-tobacco use disorder, primary current diagnosis of attention-deficit/hyperactivity disorder or major depressive disorder, (4) current tobacco or alcohol use disorder, (5) suicidal ideation with acute risk, (6) current use of psychotropic medication, (7) colorblindness, (8) visual impairment that cannot be corrected with lenses, and (9) hearing impairment. In order to isolate variation related specifically to anxiety, the broader study restricted participation to either individuals without major psychopathology or individuals with an anxiety disorder but without significant externalizing psychopathology. The institutional review board at Yale University approved all study procedures. Participants provided informed written consent to participate in the study, which entailed two visits. Participants completed the Dimensional Inventory of Stress and Trauma across

Table 1 | Demographic information

	Data not included in symptom analyses (*n* = 15)	Data included in symptom analyses (*n* = 105)	Total (*n* = 120)
Age at scan			
Mean (SD)	22.090 (2.877)	23.011 (3.177)	22.896 (3.145)
Range	18.062–27.349	18.136–30.281	18.062–30.281
Age at DISTAL			
Mean (SD)	22.005 (2.865)	22.952 (3.166)	22.834 (3.134)
Range	18.048–27.193	18.125–30.109	18.048–30.109
Sex at birth			
Female	10 (66.7%)	69 (65.7%)	79 (65.8%)
Male	5 (33.3%)	36 (34.3%)	41 (34.2%)
Gender identity			
Cisgender female	10 (66.7%)	68 (65.4%)	78 (65.5%)
Cisgender male	5 (33.3%)	35 (33.7%)	40 (33.6%)
Transgender female	0 (0.0%)	0 (0.0%)	0 (0.0%)
Transgender male	0 (0.0%)	1 (1.0%)	1 (0.8%)
Missing data	0	1	1
Education			
High school	2 (13.3%)	14 (13.3%)	16 (13.3%)
College	12 (80.0%)	69 (65.7%)	81 (67.5%)
Graduate school	1 (6.7%)	22 (21.0%)	23 (19.2%)
Total Household Income			
<$5000	0 (0.0%)	5 (4.8%)	5 (4.5%)
$5000-$11,999	0 (0.0%)	7 (6.7%)	7 (6.4%)
$12,000-$14,999	0 (0.0%)	5 (4.8%)	5 (4.5%)
$15,000-$24,999	2 (40.0%)	8 (7.6%)	10 (9.1%)
$25,000-$34,999	0 (0.0%)	10 (9.5%)	10 (9.1%)
$35,000-$49,999	0 (0.0%)	9 (8.6%)	9 (8.2%)
$50,000-$74,999	1 (20.0%)	24 (22.9%)	25 (22.7%)
$75,000-$99,999	0 (0.0%)	5 (4.8%)	5 (4.5%)
$100,000+	2 (40.0%)	32 (30.5%)	34 (30.9%)
Missing data	10	0	10
Race and ethnicity			
Asian	0 (0.0%)	26 (25.0%)	26 (22.0%)
Black or African-American	3 (21.4%)	12 (11.5%)	15 (12.7%)
Hispanic or Latinx	1 (7.1%)	12 (11.5%)	13 (11.0%)
Multiracial	1 (7.1%)	7 (6.7%)	8 (6.8%)
Non-Hispanic White	9 (64.3%)	46 (44.2%)	55 (46.6%)
Prefer not to answer	0 (0.0%)	1 (1.0%)	1 (0.8%)
Missing data	1	1	2
SCAARED anxiety symptoms			
Mean (SD)	23.300 (18.726)	26.829 (15.338)	26.522 (15.598)
Range	2.000–63.000	3.000–72.000	2.000–72.000
Missing data	5	0	5
Site			
Brain Imaging Center	7 (46.7%)	37 (35.2%)	44 (36.7%)
Magnetic Resonance Research Center	8 (53.3%)	68 (64.8%)	76 (63.3%)

Demographic information for participant sample stratified by whether participants were included in symptom analyses. *DISTAL* Dimensional Inventory of Stress and Trauma Across the Lifespan, *SCAARED* Screen for Adult Anxiety Related Disorders.

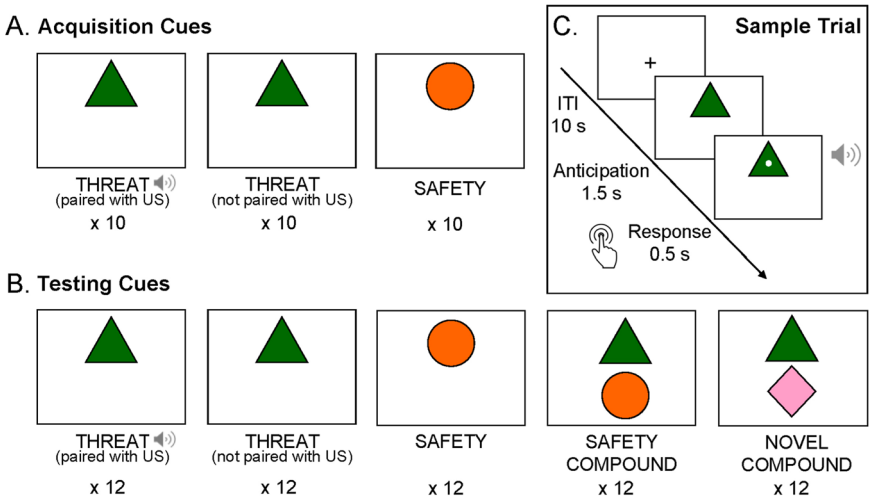

Fig. 1 | Threat and safety learning task design. Figure included with permission from a previous publication[76]. **A** During the acquisition phase of the task, participants were exposed to 10 threat cues paired with the unconditioned stimulus (US), 10 threat cues that were not paired with the US, and 10 trials of the safety cue. **B** The two testing phases of the task each included 6 threat trials paired with the US, 6 threat trials not paired with the US, 6 trials of the safety cue, 6 trials of the safety compound, and 6 trials of the novel compound (i.e., a total of 12 trials for each condition across both runs). **C** Example trial structure: a fixation cross is presented for 10 s, followed by presentation of the cue for 1.5 s, followed by 0.5 s in which a white dot appears at the center of the shape and participants are instructed to press a button.

the Lifespan (DISTAL)[67] interview as well as self-reported questionnaires assessing demographic information and mental health symptoms during the first visit. Interview data and self-report questionnaires were entered into a secure online database[68]. Participants also completed an MRI scan session with sequences including anatomical scans and functional imaging scans during the second visit. Participants were financially compensated for their time and participation at each visit. Analyses conducted in the present study were not preregistered.

Assessment of adversity exposure

Participants completed the DISTAL interview[67], which is broadly based on the structure of the UCLA PTSD Reaction Index[69] and is designed to assess key dimensions of adverse exposures including age of exposure[67]. In the screening portion of the DISTAL, participants were asked about their exposure to 24 distinct types of adverse events. For each type of adverse event that was endorsed in the screening portion of the interview, participants were asked to report on the cumulative list of ages at which they experienced that type of adversity (possible ages of exposure ranged from 0 to 30, or 0 through participant age at the time of the study, if their current age was less than 30). If multiple events of the same type were reported, age of exposure at each event was recorded. Interview data underwent extensive quality assurance and were double-entered by a team of trained research assistants, overseen by a clinical doctoral student and the principal investigator[67]. Following quality assurance, exposures to adversity were summed by individual to derive a total count of adverse events at each year of age from 0 through the participant's age at the time of the study. Subsequently, these data were summed to produce four separate variables representing counts of adverse events experienced within four developmental stages: early childhood (ages 0–5), middle childhood (ages 6–12), adolescence (ages 13–17), and adulthood (ages 18–30, or through current age), consistent with prior work[70]. Any reported events that did not include information on age of exposure were excluded from the analysis ($n = 30$ events; 1.52% of total reported events).

Clinical symptoms

Participants completed questionnaires assessing anxiety-related, trauma-related, and externalizing symptoms. Specifically, anxiety symptoms were evaluated using the total score from the Screen for Adult Anxiety Related Disorders (SCAARED)[71]. To determine the extent to which any findings might be specific to anxiety, we examined associations with trauma-related symptoms and externalizing symptoms as well. Trauma-related symptoms were assessed using the total score from the Trauma Symptoms Checklist (TSC-40)[72]. Externalizing symptoms were assessed via the Externalizing Problems subscale of the Adult Self Report scale[73].

MRI scanning

Participants were scanned on 3T Siemens Magnetom Prisma scanners (Siemens, Erlangen, Germany) using a 32-channel head coil at either the Magnetic Resonance Research Center ($n = 76$; New Haven, CT) or the Brain Imaging Center ($n = 44$; New Haven, CT). Both scanning centers used Siemens software version VE11C. Scanning sequences were based on those used in the Adolescent Brain Cognitive Development Study[74]. A whole-brain high-resolution T1-weighted anatomical scan with magnetization-prepared rapid acquisition gradient echo (MPRAGE; 1070 ms TI, 2500 ms TR; 2.9 ms TE; 8° flip angle; 256 mm field of view (FoV); 176 slices in sagittal plane; 2× parallel imaging; 1.0 × 1.0 × 1.0 mm resolution) was collected. For the threat and safety learning task, high spatial and temporal resolution multiband echo planar imaging (EPI) fMRI scans were collected with fast integrated distortion correction across a total of five runs. Sixty axial slices covering the whole brain were imaged using a T2*-weighted EPI sequence (800 ms TR; 30 ms TE; 52° flip angle; 216 mm FoV; 90 × 90 matrix; 2.4 × 2.4 × 2.4 mm resolution; 6 multiband acceleration factor with interleaved acquisition). The first 8 volumes for each task run were discarded for longitudinal magnetization to reach equilibrium. To permit accurate spatial distortion correction, two spin echo EPI scans with opposite phase encoding directions were collected prior to each block of functional scans, per Human Connectome Project (HCP) guidelines[75].

Task design

The threat and safety learning task employed in this study has been previously described[76–78]. All conditioned stimuli used in the task were geometric shapes of different colors, and the unconditioned stimulus (US) was an aversive metallic white noise[79] delivered at 95 to 100 decibels through MRI-safe noise-cancelling headphones. Briefly, the task involved five runs: acquisition, testing (two runs), extinction, and reversal (depicted in Fig. 1). The acquisition phase consisted of 20 trials of the threat cue (CS+), which were reinforced with the unconditioned stimulus (US) 50% of the time (i.e., 10 reinforced and 10 non-reinforced threat cue trials) and 10 trials of the safety cue, which was never paired with the US. The acquisition phase utilized a block format, such that all threat cues were presented sequentially, as were all safety cues. The testing phase was split into two separate but consecutive runs (~7 min each) to reduce excessive motion that may occur during longer fMRI scans. Across both runs of the testing phase, a total of 12 threat cues were paired with the US, 12 threat cues were not paired with the US, and 12 safety cues were presented. Two additional conditions were included in the testing phase of the task: a "safety compound" condition in which the threat and safety cues were presented simultaneously to test whether the safety cue transferred to reduce fear to the threat cue, and a "novel compound" condition in which the threat cue and a novel cue were

shown simultaneously to rule out effects of external inhibition[80]. Neither the safety compound nor novel compound condition was analyzed in the present study. The testing phase utilized an event-related design, and trial order was fully randomized across 6 counterbalanced versions. During every run, each cue was presented for 1500 ms and after 1000 ms a white dot appeared in the center of the shape (presented for 500 ms). Participants were instructed to press a button when the dot appeared on each trial. Participants were informed that pressing the button was simply to ensure that they were paying attention during the task. For reinforced trials of the threat cue, the onset of the aversive noise and presentation of the dot in the center of the shape were fully paired, such that they onset, lasted 500 ms, and terminated at the same time. A fixed inter-trial interval of 10 s separated each trial to allow for stabilization of the skin conductance response (SCR) signal. The assignment of the three different shapes used to cue the three stimulus types (threat, safety, or novel cue) was counterbalanced across participants. Counterbalanced task version did not relate to any variables of interest or latent profile assignment (see Supplementary Results). Additional details on the extinction and reversal runs of the task can be found in the original paper[77]. In the present study, we examined non-reinforced threat cues and safety cues during the two testing runs in fMRI analyses, and non-reinforced threat cues and safety cues during the acquisition block as well as during the two testing runs to evaluate cue learning via SCR. Details on SCR processing and analyses indicating that participants successfully learned the task cues can be found in the Supplementary Methods and Results.

fMRI preprocessing

fMRI data were converted to Brain Imaging Data Structure (BIDS)[81] using *heudiconv* (https://github.com/nipy/heudiconv) and subsequently preprocessed using the HCP minimal preprocessing pipeline[75] using the HCP Pipelines BIDS app (https://github.com/BIDS-Apps/HCPPipelines) version 3.17.14. This pipeline has been described in detail in previous work[76–78]. Briefly, preprocessing of task-based functional acquisitions involved gradient distortion correction, EPI "fieldmap" preprocessing and distortion correction, motion correction, nonlinear registration to the MNI template (MNI 152, 2 mm space), and grand-mean intensity normalization. The EPI fMRI images were corrected using spin echo fieldmap EPI scans with opposite phase encoding directions, resulting in opposite spatial distortion. The two fieldmap images were aligned using nonlinear optimization to estimate the distortion field and enable the removal of spatial and intensity distortions from the fMRI images via the HCP minimal preprocessing pipeline[82–84].

fMRI first level analysis

All individual-level fMRI analyses were conducted with the FMRIB's Software Library (FSL) version 6.0.7.9. For the first-level FEAT analysis, predictors for all task conditions (threat cue, safety cue, safety compound, and novel compound conditions; with inter-trial intervals treated as baseline) were convolved with a double-gamma canonical hemodynamic response function (HRF). To minimize the effects of motion on task-related results, each participant's FEAT design matrix had translational and rotational motion parameters, resulting from FSL's MCFLIRT[85], added as nuisance regressors. Additionally, FSL's *fsl_motion_outliers* function was used to detect fMRI frames that were corrupted by excessive motion and were therefore less reliable; outliers were determined using 1.5 times the interquartile range above the upper quartile[86] and the mean framewise displacement (FD) was calculated[87]. The resulting outlier frame regressors (encoded as one-hot vectors indicating the presence or absence of an outlier) were then concatenated to the design matrix. We chose to employ this approach rather than censoring corrupted timepoints because regression of problematic timepoints does not disrupt the temporal structure of the timeseries. Temporal derivatives of all design matrix predictors were added as confound terms to the GLM to account for slice-timing differences and variability in the HRF delay across regions. Finally, timeseries were high-pass filtered with a cutoff of 90 s (estimated for our specific task design using FSL's *cutoffcalc* function) to remove low frequency artifacts and pre-whitened with FILM to correct for autocorrelations in the timeseries.

Region of interest (ROI) extraction and covariate regression

Voxel-level parameter estimates produced in FSL from the first-level analyses of the first and second testing runs were averaged together using the *fslmaths* command[88] to yield estimates of average activation for the three contrasts of interest (threat vs. baseline, safety vs. baseline, and threat vs. safety). Global mean activation was computed per participant for each contrast at the voxel level using the *fslmaths* command. Given the canonical role of the vmPFC, dACC, hippocampus, and amygdala in threat and safety learning and response[89–91], we selected ROIs representing these key nodes to submit to LPA. Specifically, we derived anatomical segmentations of the bilateral hippocampus and amygdala from the Shen 368 atlas[92], bilateral ventromedial prefrontal regions from the symmetrical Mackey vmPFC atlas[93], and the bilateral dACC region from the Automated Anatomical Labeling Atlas 3[94] as in previous work[76,78]. All ROIs were averaged across hemispheres to increase model parsimony and because we did not have specific hypotheses regarding lateralization.

Quality assessment and motion exclusion

Following preprocessing, all data were visually inspected for artifacts by a highly trained team of research assistants. Subjects with task runs with severe artifacts (e.g., severe motion slice, signal distortion, etc.) were excluded from analysis. Given the well-documented impacts of motion on fMRI signal[95], we employed rigorous motion correction during FEAT first level analysis, as previously described. In addition, we included mean framewise displacement across both task runs as a between-subjects covariate[96,97]. Finally, we inspected overlap between areas with fMRI artifacts and ROIs. Mackey atlas nodes 14m, 24, 25, and 32 were included in subsequent analyses, while nodes 11m, 14c, 14r, and 14rr were excluded (across all participants) due to overlap with artifacts.

Data preparation and outlier removal

We employed LPA[64,65] to identify person-centered profiles characterized by shared patterns of adversity exposure across development and neural discrimination between threat and safety cues. Prior to submitting adversity and neural indicator variables to the LPA model, we regressed between-subjects covariates from each measure. Specifically, from each of the four adversity exposure variables (representing exposures in early childhood, middle childhood, adolescence, and adulthood) we regressed age at DISTAL interview and sex assigned at birth using a zero-inflated negative binomial model implemented in *statsmodels*[98]. For neural data, we regressed estimated total intracranial volume, site of fMRI scan acquisition, mean framewise displacement, mean whole-brain activation, and age at scan session from each ROI's activation using ordinary least squares (OLS) models implemented in *statsmodels*[98]. We performed covariate regression from ROI activation data separately for each contrast of interest (threat vs. baseline, safety vs. baseline, and threat vs. safety). We chose to regress mean whole-brain activation to isolate region-specific variation in activation while controlling for global individual differences, and total intracranial volume to account for both variability in head size and as a proxy for potential sex-related differences[99]. Prior to fitting the LPA model, we tested for the presence of outliers in each variable (i.e., more than 3 standard deviations from the median), and excluded participants with any data surpassing this threshold ($n = 11$; original sample $n = 131$, final sample $n = 120$). Subsequently, we tested for multicollinearity among all adversity exposure and neural indicator variables using the variance inflation factor (VIF). Activation in Mackey areas 14m and 32 were highly correlated, leading us to average their activations and use this combined variable in subsequent analyses. Following this step, VIFs for all variables were less than 5, indicating that variables were not problematically multicollinear[100]. Finally, all indicator variables were z-scored prior to submission to the LPA model.

Latent profile analysis

Statistical analyses were conducted in Python (version 3.9)[101], and R (version 4.4.2)[102]. A full list of python package versions can be found in the project Github repository (see *Data and Code Availability)*. LPA was implemented in the Python package StepMix[103], a mixture modeling package that introduces advanced features such as bias correction that have previously been predominantly unavailable in open-source software. The following variables were entered into the LPA: adversity count during early childhood, adversity count during middle childhood, adversity count during adolescence, adversity count during adulthood, hippocampal activation during the threat vs. safety contrast, amygdala activation during the threat vs. safety contrast, vmPFC area 24 activation during the threat vs. safety contrast, vmPFC area 25 activation during the threat vs. safety contrast, vmPFC areas 32 and 14m activation during the threat vs. safety contrast, and dACC activation during the threat vs. safety contrast. LPA models treating all variables as continuous with diagonal component covariance structures were fit across 1000 random starts for 1 through 6 latent profiles, and information criteria were retained for each model fit and compared. We chose to limit the maximum number of profiles to 6, as prior work suggests that with sufficient separation, the minimum expected sample per latent profile should be $n = 20$[104]. Thus, with $n = 120$, the maximum number of profiles we would be powered to detect is 6. Models were fit using the three-step method, and profile assignment was corrected using the Bolck, Croon, and Hagenaars (BCH) method[64,103,105]. The optimal profile number was selected by comparing fit based on information criteria. We employed the Bayesian Information Criterion (BIC)[106] and the Akaike Information Criterion (AIC)[107], both of which indicate better fit with values ranging closer to zero; and scaled entropy, in which higher values indicate higher classification confidence and values above 0.8 are considered acceptable[103,108]. After selecting the optimal profile solution based upon information criteria values, we confirmed a superior fit for the chosen solution with k latent profiles relative to the solution with k-1 profiles using 1000 iterations of a bootstrapped likelihood ratio test[109]. Participants were assigned profile membership, and the categorical variable representing profile membership was used in subsequent analyses with clinical symptoms. Finally, we ordered the profiles from least to most cumulative adversity exposure for ease of interpretation. Post-hoc tests for differences between profiles in adversity exposure across development were evaluated using two-tailed Mann–Whitney U-Tests[110], and False Discovery Rate (FDR)[111] correction was applied to account for multiple comparisons (i.e., the three pairwise tests comparing each pair of profiles). Differences between profiles in normally distributed data (e.g., neural activation and clinical symptoms) were evaluated with pairwise Games-Howell tests[112]. Differences in neural discrimination between threat and safety within profiles were evaluated relative to zero using one-sample t-tests and corrected for multiple comparisons using FDR correction. Post-hoc testing was implemented in the *pingouin* Python package[113].

Statistical power considerations

Following latent profile identification, we sought to confirm that we were well-powered to identify the correct number of latent profiles in our sample. As distance between profiles may be more important than sample size in determining statistical power[104,114,115], we indexed distance between profiles using two approaches. First, in line with previous work[115], we computed pairwise Cohen's d effect sizes between latent profiles for each variable submitted to the LPA model. We then computed the absolute value of each Cohen's d value and averaged across each pairwise combination of latent profiles to determine the overall distance (average Cohen's d) between the profiles[115]. Second, we computed a more recently proposed measure of separation—the distance metric (Δ)[104]. Specifically, we again retained Cohen's d values representing the pairwise differences between profiles that were computed during pairwise testing for each of the 10 indicator variables submitted to the LPA model (exposure to adversity during early childhood, exposure to adversity during middle childhood, exposure to adversity during adolescence, exposure to adversity during adulthood, hippocampal activation during the threat vs. safety contrast, amygdala activation during the threat vs. safety contrast, vmPFC area 24 activation during the threat vs. safety contrast, vmPFC area 25 activation during the threat vs. safety contrast, vmPFC areas 32 and 14m activation during the threat vs. safety contrast, and dACC activation during the threat vs. safety contrast). We then squared each Cohen's d value and summed the squares together for each pair of profiles (1 vs. 2, 1 vs. 3, 2 vs. 3). We computed the square root of the sum of squares between each pair of profiles, and then averaged these values together to obtain an overall estimate of distance between profiles.

Associations with clinical symptoms

Following profile assignment, we examined associations between profile membership and measures of clinical symptoms. We used the Jarque–Bera (JB) test[116] to test whether symptom variables met assumptions of normality. None of the symptom measures (anxiety symptoms, trauma-related symptoms, externalizing symptoms) met the assumption of normality; thus, anxiety symptoms were transformed using a square-root transform and trauma-related and externalizing symptoms were transformed using a log transform. Transformations were chosen for each symptom variable based upon which transformation resulted most closely in an approximately normal distribution (i.e., JB>0.05). Next, transformed anxiety symptoms, transformed trauma-related symptoms, and transformed externalizing symptoms were evaluated as dependent variables in separate OLS models fit using lm() in R[102]. Age at questionnaire completion, sex assigned at birth, total household income, and years of education were included as covariates in all models. We chose to include age at questionnaire completion and sex assigned at birth as covariates in each model to adjust for potential age-related differences in symptom measures[117] and given prior evidence of sex differences in the effects of adversity on neurodevelopment and mental health[118,119]. We included total household income and years of education as proxies for socioeconomic status-related experiences that can impact brain development[120,121] and mental health[3,119]. Participants with missing data for any covariates were excluded from symptom analyses ($n = 15$; Table 1). Type III Sum of Squares ANOVA tables were then computed for each fit OLS model to ascertain the effect of the categorical latent profile variable relative to the grand mean[122] using the *car* package in R[123]. We chose to employ "effects coding" in this manner given the lack of a clear reference group among the three profiles. Subsequently, pairwise differences between profiles were assessed using Games-Howell tests, implemented via the *rstatix* package in R[112,124]. We applied FDR correction for multiple comparisons to account for the three symptom models. Independent of the OLS models, Spearman correlations were fit to determine whether the clinical measures correlated with the covariates for continuous measures. Correlations among clinical symptom measures, covariates, and LPA indicator variables of interest are presented in Fig. S1.

Sensitivity analyses

In order to parse the relative contribution of cumulative adversity exposure in the present findings, we conducted two sensitivity analyses. First, we refit the LPA modeling pipeline using a single variable indexing cumulative lifetime adversity exposure instead of the four variables indexing the count of adversity exposures within each developmental stage. This single variable was submitted alongside the neural variables to the LPA model (hippocampal activation during the threat vs. safety contrast, amygdala activation during the threat vs. safety contrast, vmPFC area 24 activation during the threat vs. safety contrast, vmPFC area 25 activation during the threat vs. safety contrast, vmPFC areas 32 and 14m activation during the threat vs. safety contrast, and dACC activation during the threat vs. safety contrast). We compared information criteria to determine the best-fitting profile solution and then ordered the resulting profiles from least to most cumulative adversity exposure to facilitate profile assignment comparison between the present model and our original model. We then computed a Spearman correlation between the present profile assignments and the profile assignments from the original analysis to quantify similarity. Second, we sought to determine whether cumulative adversity exposure displayed a quadratic association with anxiety symptoms, as would be expected if the

anxiety-related differences between profiles were primarily driven by cumulative adversity exposure. We fit an OLS regression model using transformed anxiety symptoms from the SCAARED questionnaire as the dependent variable, the sum score of cumulative adverse events (modeled as a quadratic polynomial term) as the primary independent variable of interest, and sex assigned at birth, age at questionnaire completion, total household income, and total years of education as covariates. We then examined the OLS results using a type III Sum of Squares ANOVA table to maintain consistency with previous analyses.

Results

LPA model fitting results

We fit a latent profile model using both neural and adversity exposure data across development and evaluated solutions for models fit with the number of latent profiles ranging from 1 to 6. Information criteria for each of these solutions is presented in Table 2. Based upon the BIC, the optimal number of profiles was determined to be k=3 (BIC=3364.296) given the superior ability of the BIC to identify the correct number of profiles relative to other information criteria[115,125]. The three-class solution also demonstrated acceptably high scaled entropy (scaled entropy = 0.903), indicating high classification confidence[108]. Using 1000 iterations of the bootstrapped likelihood ratio test, we confirmed that the three-profile solution demonstrated superior fit relative to the two-profile solution (p = 0.004).

Statistical power

Next, we sought to confirm that we were adequately powered for the BIC to reliably detect the class solution using two separate methods. First, we computed distance between classes (i.e., average Cohen's d) to assess statistical power. The average Cohen's d between profiles 1 and 2 was 1.144, the average Cohen's d between profiles 1 and 3 was 1.085, and the average Cohen's d between profiles 2 and 3 was 0.723. This yielded an overall average value of 0.984, surpassing the minimum recommended distance value of 0.8 for two out of three profiles and overall[115]. Next, we computed the distance (Δ)[104] between each pair of profiles (1 vs. 2: Δ = 4.230; 1 vs. 3: Δ = 3.814, 2 vs. 3: Δ = 2.781). Average separation across the three profiles (Δ = 3.608) surpassed the threshold for >99% power (Δ = 3)[104], suggesting that the present sample shows sufficient separation for the BIC to correctly identify the number of latent profiles. Finally, we confirmed that neither LPA profile assignment nor any of the indicator variables differed as a function of counterbalanced task version (see Supplementary Results).

Table 2 | LPA information criteria

Number of latent profiles	BIC	AIC	Scaled entropy
1	3501.202	3445.453	
2	3378.922	3264.635	0.868
3	3364.269	3191.445	0.903
4	3385.042	3153.680	0.911
5	3419.133	3129.234	0.928
6	3452.278	3103.842	0.936

Information criterion values are presented for latent profile analysis (LPA) models with up to 6 latent profiles.
BIC Bayesian Information Criterion, *AIC* Akaike Information Criterion.

Latent profile characterization

The three latent profiles differed in adversity exposure across development (Fig. 2; Table S1) and in neural activation when discriminating between threat and safety across the vmPFC, hippocampus, and amygdala (Fig. 3). Participants in latent profile 1 (n = 14) reported the fewest adverse exposures across development and had lower adversity exposure within middle childhood and adolescence than participants in latent profile 2 (ps_{FDR}<0.01; Table 3). Latent profile 1 also demonstrated higher activation in the threat vs. safety contrast specifically in regions of the vmPFC compared to latent profiles 2 and 3 (ps < 0.001; Table 3); these findings were driven by higher activation to threat cues and lower activation to safety cues (Table S2). Participants in latent profile 2 (n = 66) reported a moderate number of adverse exposures across development that were increased relative to latent profile 1 specifically within middle childhood and adolescence (ps_{FDR} = 0.001; Table 3). Latent profile 2 also demonstrated lower activation in the threat vs. safety contrast, which differed from latent profile 1 in all regions except for the dACC (ps < 0.01; Table 3) and from latent profile 3 specifically in the hippocampus and amygdala (ps < 0.01; Table 3). Lower activation in the threat vs. safety contrast in latent profile 2 was predominantly driven by lower activation to threat in all regions (particularly the hippocampus and amygdala) and higher activation to safety in the vmPFC relative to latent profile 1 (Table S2). Participants in latent profile 3 (n = 40) reported the highest number of adverse exposures across development, with higher adversity exposure within all developmental stages than latent profiles 1 and 2 (ps_{FDR}<0.01; Table 3). In addition, participants in latent profile 3 demonstrated activation values close to zero in the threat vs. safety contrast, driven by low neural activation to both threat and safety cues in all regions (Fig. 3). Compared to latent profile 2, latent profile 3 showed higher activation to threat specifically in the hippocampus and amygdala (ps < 0.05; Table S2). Descriptive statistics for adversity exposure by latent profile are reported in Table S1, and full statistics for pairwise tests used to characterize differences between latent profiles in indicator variables are presented in Table 3. Statistics for between-profile differences in the threat vs. baseline and safety vs. baseline contrasts are presented in Table S2. Demographic information for each profile is presented in Table S3.

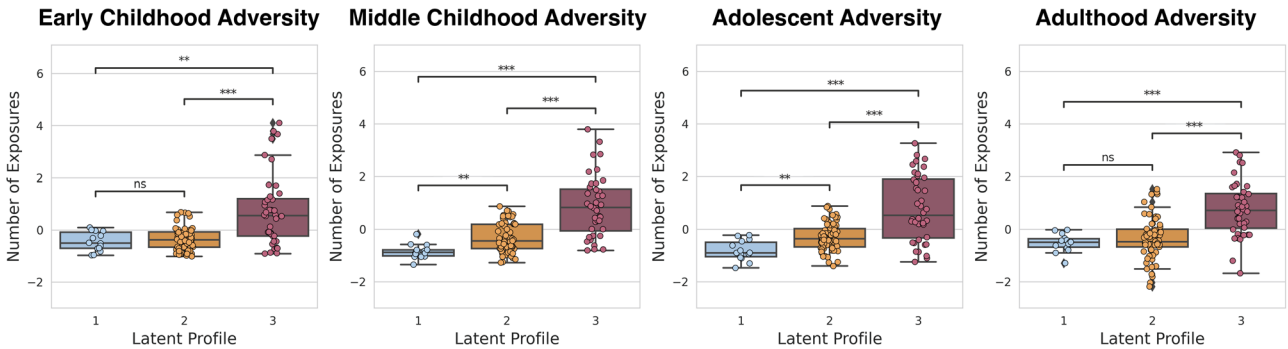

Fig. 2 | Differences between latent profiles (n = 14 in profile 1; n = 66 in profile 2; n = 40 in profile 3) in adversity exposure within each developmental stage are presented. Mann–Whitney U-tests with FDR correction were used. The adversity exposure measures presented here are standardized residuals obtained following covariate regression. In this figure, the box shows the data quartiles and the whiskers show the data range. Points that are determined to be "outliers" using the interquartile range method are plotted outside the whiskers. ns not significant; *p < 0.05; **p < 0.01; ***p < 0.001.

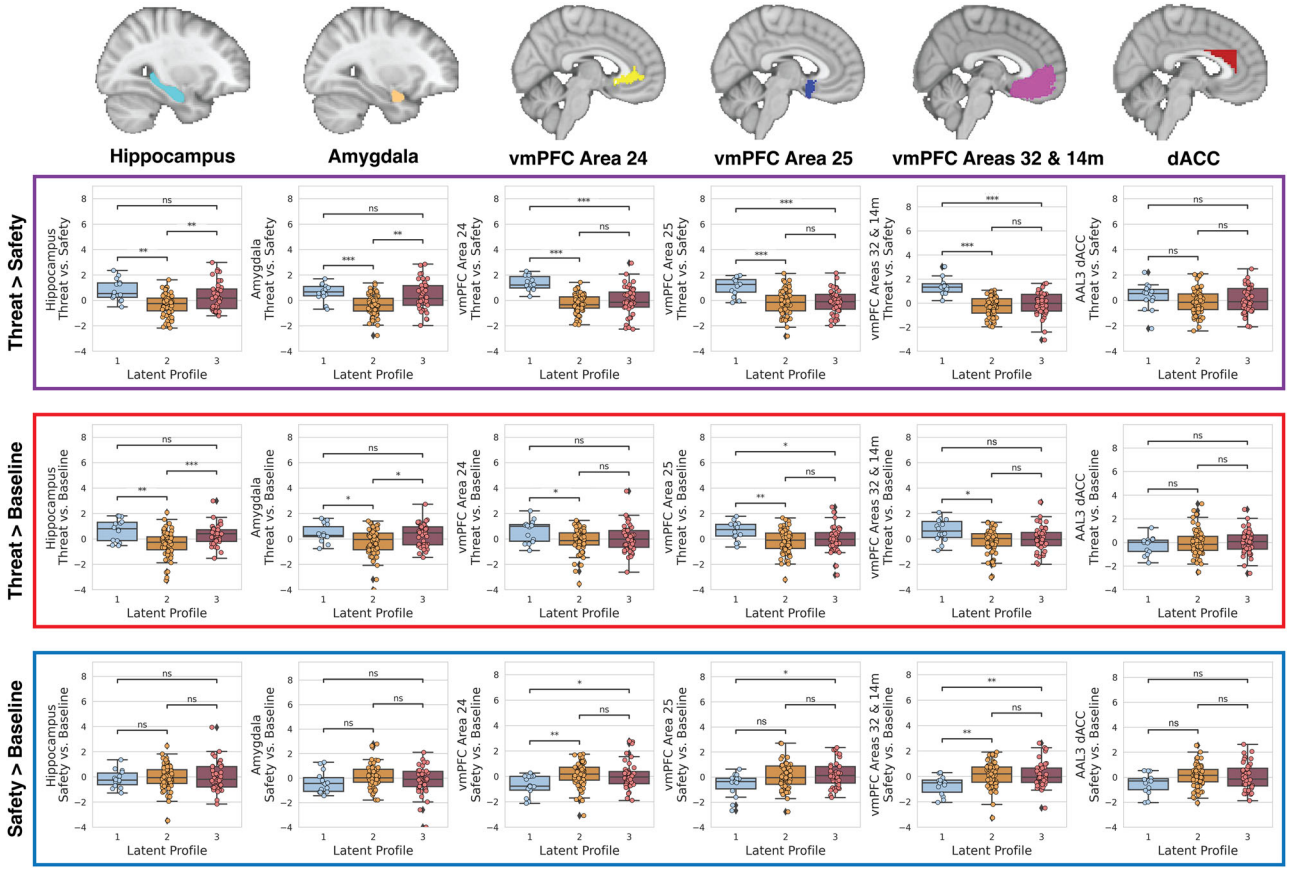

Fig. 3 | Differences between latent profiles ($n = 14$ in profile 1; $n = 66$ in profile 2; $n = 40$ in profile 3) in neural activation are presented. Games-Howell post-hoc tests were used to determine whether activation differed across profiles for each ROI and contrast. The threat vs. safety contrast is presented in the first row, the threat vs. baseline contrast is presented in the second row, and the safety vs. baseline contrast is presented in the third row. The neural activation measures shown here are standardized residuals obtained following covariate regression. In this figure, the box shows the data quartiles and the whiskers show the data range. Points that are determined to be "outliers" using the inter-quartile range method are plotted outside the whiskers. ns = not significant; $^{*}p < 0.05$; $^{**}p < 0.01$; $^{***}p < 0.001$.

Differences in neural discrimination within each profile

Next, we sought to formally test whether individuals within each latent profile displayed differential activation to threat and safety cues (i.e., whether individuals were neurally discriminating between threat and safety). To do this, we conducted two-tailed one-sample *t*-tests *within each latent profile* to evaluate whether neural activation in the threat vs. safety contrast differed statistically from zero. Statistics are presented in Table 4. Overall, neural activation in the threat vs. safety contrast in latent profile 1 differed from zero in all neural regions except the dACC ($ps_{FDR} < 0.05$; Table 4), suggesting individuals in this profile discriminated between threat and safety cues. Neural activation in latent profile 2 also differed from zero in all neural regions except for vmPFC area 24 and the dACC ($p_{FDR} < 0.05$; Table 4). However, neural activation in the threat vs. safety contrast in latent profile 3 did not differ statistically from zero in any of the ROIs examined ($ps_{FDR} > 0.05$; Table 4).

Associations with clinical symptoms

Finally, we used OLS models to examine differences between latent profiles in anxiety symptoms, trauma-related symptoms, and externalizing symptoms. The omnibus model for anxiety symptoms was significant ($F(20, 84) = 1.740$, $p = 0.042$), and the main effect of latent profile on anxiety symptoms was significant ($F(2) = 4.404$, $p = 0.015$). Post-hoc Games–Howell tests revealed that latent profile 1 ($M = 5.762$, SD = 1.030) had significantly higher anxiety symptoms than latent profile 2 ($M = 4.692$, SD = 1.403; mean difference = –1.000, SE = 0.243, 95% CI = [–1.865, –0.134], $p = 0.022$, $d = 0.811$, 95% CI_d = [0.317, 1.380]). Latent profile 2 ($M = 4.692$, SD = 1.403) also displayed significantly lower anxiety symptoms than latent profile 3 ($M = 5.461$, SD = 1.527; mean difference = 0.821, SE = 0.226, 95% CI = [0.057, 1.586], $p = 0.032$, $d = –0.539$, 95% CI_d = [–0.931, –0.043]), but there was no statistically significant evidence that latent profiles 1 and 3 differed in anxiety symptoms (mean difference = –0.178, SE = 0.283, 95% CI = [–1.162, 0.806], $p = 0.897$, $d = 0.128$, 95% CI_d = [–0.300, 0.799]; Fig. 4). Omnibus models were not significant for trauma-related symptoms

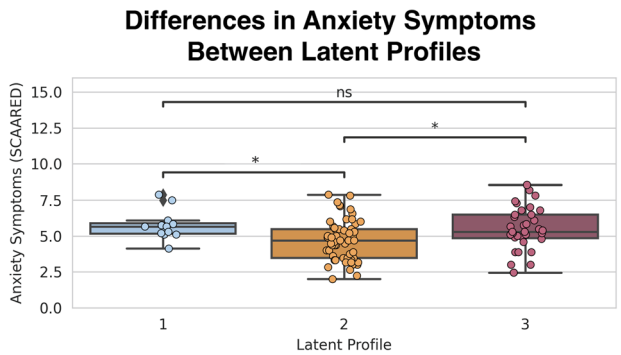

Fig. 4 | Games-Howell post-hoc tests yielded differences in anxiety symptoms between latent profiles 1 and 2 and between latent profiles 2 and 3 ($n = 12$ in profile 1; $n = 58$ in profile 2; $n = 35$ in profile 3). In this figure, the box shows the data quartiles and the whiskers show the data range. Points that are determined to be "outliers" using the inter-quartile range method are plotted outside the whiskers. ns not significant; $^{*}p < 0.05$; $^{**}p < 0.01$; $^{***}p < 0.001$.

Table 3 | Differences between profiles

	Early childhood adversity			Middle childhood adversity			Adolescence adversity			Adulthood adversity			Hippocampal activation (Threat vs. safety)			Amygdala activation (Threat vs. safety)			vmPFC area 24 activation (Threat vs. safety)			vmPFC area 25 activation (Threat vs. safety)			vmPFC areas 32 and 14m activation (Threat vs. safety)			dACC activation (Threat vs. safety)		
Latent classes (A vs. B)	**1 vs. 2**	**1 vs. 3**	**2 vs. 3**	**1 vs. 2**	**1 vs. 3**	**2 vs. 3**	**1 vs. 2**	**1 vs. 3**	**2 vs. 3**	**1 vs. 2**	**1 vs. 3**	**2 vs. 3**	**1 vs. 2**	**1 vs. 3**	**2 vs. 3**	**1 vs. 2**	**1 vs. 3**	**2 vs. 3**	**1 vs. 2**	**1 vs. 3**	**2 vs. 3**	**1 vs. 2**	**1 vs. 3**	**2 vs. 3**	**1 vs. 2**	**1 vs. 3**	**2 vs. 3**	**1 vs. 2**	**1 vs. 3**	**2 vs. 3**
Mean (A)	−0.451	−0.451	−0.353	−0.850	−0.850	−0.340	−0.819	−0.819	−0.299	−0.524	−0.524	−0.345	0.813	0.813	−0.347	0.639	0.639	−0.357	1.358	1.358	−0.262	1.087	1.087	−0.174	1.450	1.450	−0.259	0.304	0.304	−0.096
SD (A)	0.368	0.368	0.433	0.272	0.272	0.548	0.381	0.381	0.519	0.341	0.341	0.812	0.851	0.851	0.823	0.659	0.659	0.819	0.567	0.567	0.716	0.714	0.714	0.960	0.816	0.816	0.785	1.059	1.059	0.967
Mean (B)	−0.353	0.740	0.740	−0.340	0.859	0.859	−0.299	0.779	0.779	−0.345	0.753	0.753	−0.347	0.288	0.288	−0.357	0.366	0.366	−0.262	−0.043	−0.043	−0.174	−0.093	−0.093	−0.259	−0.081	−0.081	−0.096	0.053	0.053
SD (B)	0.433	1.369	1.369	0.548	1.158	1.158	0.519	1.251	1.251	0.812	1.029	1.029	0.823	1.087	1.087	0.819	1.146	1.146	0.716	1.156	1.156	0.960	0.941	0.941	0.785	0.976	0.976	0.967	1.045	1.045
Test statistic	410.000	116.000	608.500	188.000	20.000	454.500	191.000	66.000	651.000	407.000	50.000	489.000	4.659	1.839	−3.187	4.911	1.083	−3.486	9.245	5.903	−1.075	5.619	4.875	−0.430	7.164	5.729	−0.977	1.302	0.765	−0.732
p-value (corrected)	0.514	**0.002**	**<0.001**	**0.001**	**<0.001**	**<0.001**	**0.001**	**<0.001**	**<0.001**	0.490	**<0.001**	**<0.001**	**0.001**	0.175	**0.006**	**<0.001**	0.530	**0.003**	**<0.001**	**<0.001**	0.533	**<0.001**	**<0.001**	0.903	**<0.001**	**<0.001**	0.594	0.412	0.728	0.745
Cohen's *d*	−0.232	−0.992	−1.206	−0.995	−1.689	−1.443	−1.043	−1.453	−1.240	−0.238	−1.408	−1.221	1.402	0.508	−0.683	1.253	0.262	−0.757	2.337	1.346	−0.241	1.365	1.326	−0.086	2.163	1.631	−0.207	0.407	0.239	−0.149
Bootstrapped 95% CI (Cohen's *d*)	[−0.727, 0.286]	[−1.275, −0.652]	[−1.642, −0.836]	[−1.358, −0.571]	[−2.132, −1.296]	[−1.864, −0.985]	[−1.479, −0.537]	[−1.921, −1.014]	[−1.741, −0.732]	[−0.547, 0.141]	[−1.885, −0.841]	[−1.689, −0.763]	[0.827, 2.024]	[−0.097, 1.131]	[−1.042, −0.28]	[0.591, 1.728]	[−0.259, 0.760]	[−1.152, −0.299]	[1.749, 2.956]	[0.787, 1.863]	[−0.695, 0.249]	[0.814, 1.883]	[0.720, 1.954]	[−0.479, 0.299]	[1.556, 2.717]	[1.092, 2.163]	[−0.619, 0.250]	[−0.340, 1.057]	[−0.464, 0.842]	[−0.569, 0.242]

Differences between profiles for developmental adversity variables were evaluated using Mann–Whitney U-Tests with FDR correction, while neural activation differences between profiles in the threat vs. safety contrast for each ROI were assessed using Games–Howell post-hoc tests. The neural variables presented here are standardized residuals obtained following covariate regression. Profile membership: n = 14 in profile 1; n = 66 in profile 2; n = 40 in profile 3 for all variables submitted to the LPA model. Statistically significant p-values ($p < 0.05$) are in bold.

($F(20, 74) = 1.604$, $p = 0.074$) or externalizing symptoms ($F(20, 82) = 1.362$, $p = 0.166$), nor was the main effect of latent profile on either symptom measure significant (trauma-related symptoms: $F(2) = 0.396$, $p = 0.674$; externalizing symptoms: $F(2) = 2.995$, $p = 0.087$). As these models were not significant, post-hoc tests were not examined. Following multiple comparisons correction across OLS models for the three clinical symptom measures, the main effect of latent profile on anxiety symptoms survived ($p_{FDR} = 0.045$). Spearman correlations among LPA indicator variables, clinical symptom measures, and covariates are presented in Fig. S1.

Sensitivity Analyses

In order to disentangle the extent to which the present results may be driven by cumulative adversity exposure, we conducted two sensitivity analyses. First, we refit the LPA model using a single variable indexing cumulative lifetime adversity exposure instead of the four variables indexing the count of adversity exposures within each developmental stage. As in previous analyses, we relied on the BIC to indicate the correct class solution. The two-class solution showed the lowest BIC value (BIC = 2415.043; Table S4), suggesting that a two-class solution fit the data best. Class assignment in the two-class solution was weakly correlated with that of our original model (Spearman's $r = 0.211$, $p = 0.021$). Furthermore, choosing to fit a three-class solution for consistency with previous analyses (despite it not being indicated by the BIC) did not recapitulate the solution observed with the developmental adversity variables, instead showing only weak correlation with class assignment in the original model (Spearman's $r = 0.196$, $p = 0.032$). This three-class solution also did not show evidence of a statistically significant difference in anxiety symptoms across profiles ($F(2) = 0.584$, $p = 0.560$). These results suggest that cumulative exposure alone does not drive results of the present analysis, and that collapsing across developmental stage may obscure person-specific patterns of adversity exposure and neural activation that are relevant to mental health. Next, we sought to parse the extent to which the observed differences in anxiety symptoms between the profiles may be due to between-profile differences in cumulative adversity exposure rather than due to between-profile differences in the developmental timing of adversity exposure. To do this, we fit an OLS model to test whether cumulative adversity exposure showed a quadratic association with anxiety symptoms—in other words, to see if moderate adversity exposure was associated with lower anxiety, relative to lower and higher levels of adversity exposure, across the whole sample. Results did not show evidence of a significant quadratic association between anxiety symptoms and cumulative number of adverse events ($F(1) = 2.531$, $p = 0.115$). Together, these sensitivity analyses suggest that accounting for developmental stage when modeling the effects of adversity exposure may provide insight above and beyond cumulative exposure alone into heterogeneity in mental health outcomes.

Discussion

Parsing heterogeneity in neurobehavioral processes and mental health following adversity is a crucial step toward improving understanding of risk and resilience. In the present exploratory study, we leveraged a person-centered approach to identify profiles of individuals characterized by shared patterns of adversity exposure across development, from early childhood through young adulthood, and neural activation to threat and safety. Three latent profiles emerged, which displayed differences in developmental adversity exposure, neural responses during threat and safety learning, and anxiety symptoms in young adulthood. The first latent profile was characterized by lower levels of lifetime adversity exposure, higher activation to threat, and lower activation to safety. The second latent profile was characterized by moderate adversity exposure within middle childhood and adolescence, together with lower neural activation to threat and higher neural activation to safety. The third latent profile was characterized by higher levels of lifetime adversity exposure and diminished neural discrimination between threat and safety cues. Individuals in the second latent profile had the lowest levels of anxiety symptoms, whereas

https://doi.org/10.1038/s44271-025-00193-x

Table 4 | Differences in neural discrimination within each profile

	Latent profile	Contrast (A)	Mean (A)	SD (A)	*t*	Degrees of freedom	*p*-value	p_{FDR}	Cohen's *d*	Bootstrapped 95% CI (Cohen's *d*)
Hippocampal activation	**1**	Threat vs. safety	0.813	0.851	3.573	13	**0.003**	**0.005**	0.955	[0.389, 1.482]
	2	Threat vs. safety	−0.347	0.823	−3.429	65	**0.001**	**0.003**	0.422	[0.162, 0.666]
	3	Threat vs. safety	0.288	1.087	1.678	39	0.101	0.101	0.265	[0.020, 0.547]
Amygdala activation	**1**	Threat vs. safety	0.639	0.659	3.631	13	**0.003**	**0.005**	0.971	[0.293, 1.981]
	2	Threat vs. safety	−0.357	0.819	−3.541	65	**0.001**	**0.002**	0.436	[0.175, 0.649]
	3	Threat vs. safety	0.366	1.146	2.018	39	0.051	0.051	0.319	[0.048, 0.627]
vmPFC area 24 activation	**1**	Threat vs. safety	1.087	0.714	5.696	13	**<0.001**	**<.001**	1.522	[1.482, 3.092]
	2	Threat vs. safety	−0.174	0.960	−1.475	65	0.145	0.218	0.182	[0.123, 0.606]
	3	Threat vs. safety	−0.093	0.941	−0.623	39	0.537	0.537	0.098	[0.001, 0.119]
vmPFC area 25 activation	**1**	Threat vs. safety	1.358	0.567	8.968	13	**<0.001**	**<0.001**	2.397	[0.850, 2.621]
	2	Threat vs. safety	−0.262	0.716	−2.971	65	**0.004**	**0.006**	0.366	[0.009, 0.404]
	3	Threat vs. safety	−0.043	1.156	−0.238	39	0.813	0.813	0.038	[0.001, 0.310]
vmPFC areas 32 & 14m activation	**1**	Threat vs. safety	1.450	0.816	6.649	13	**<0.001**	**<0.001**	1.777	[1.222, 2.360]
	2	Threat vs. safety	−0.259	0.785	−2.678	65	**0.009**	**0.014**	0.330	[0.094, 0.561]
	3	Threat vs. safety	−0.081	0.976	−0.523	39	0.604	0.604	0.083	[0.000, 0.271]
dACC activation	**1**	Threat vs. safety	0.304	1.059	1.072	13	0.303	0.632	0.287	[0.003, 0.885]
	2	Threat vs. safety	−0.096	0.967	−0.809	65	0.421	0.632	0.100	[0.003, 0.304]
	3	Threat vs. safety	0.053	1.045	0.319	39	0.751	0.751	0.050	[0.000, 0.167]

Within each profile, one-sample *t*-tests were used to assess whether neural activation in the threat vs. safety contrast differed significantly from zero for each region of interest. The neural activation measures presented here are standardized residuals obtained following covariate regression. Statistically significant *p* values ($p < 0.05$) are in bold. Profile membership: $n = 14$ in profile 1; $n = 66$ in profile 2; $n = 40$ in profile 3 for all variables submitted to the LPA model.
ns not significant.

individuals in the first and third latent profiles had relatively higher levels of anxiety that did not statistically differ. Together, these findings suggest that both the timing and number of adversity exposures across development may be linked with distinct patterns of neural discrimination between threat and safety and that these joint patterns may be relevant for understanding anxiety risk.

The present findings add to a growing body of evidence that significant adversity exposure during development is associated with weaker neural discrimination between threat and safety cues in the context of aversive learning[30]. Specifically, we found that the co-occurrence of high lifetime adversity exposure and diminished neural threat/safety discrimination in the third latent profile was driven by blunted neural activation to both the threat and safety cues, aligning with prior evidence of blunted reactivity to threat among individuals with high levels of adversity exposure[30,32,33,40]. Interestingly, neural activation to threat in the third latent profile differed from the second latent profile––characterized by lower anxiety––in only a few brain regions. Specifically, individuals in the third latent profile showed slightly increased activation to the threat cue in the hippocampus and amygdala relative to individuals in the second latent profile. We posit that these patterns could reflect disrupted prefrontal regulation of subcortical regions in the third latent profile, or, conversely, more effective regulation of subcortical regions by the vmPFC in the second latent profile when faced with threat. Importantly, however, determining the cognitive correlates of diminished neural discrimination—i.e., whether diminished neural discrimination reflects diminished learning or an alternative process (e.g., decreased salience of both conditions despite learning)—will require additional research.

Contrary to our hypothesis that a profile would emerge with both the highest levels of adversity exposure and the highest levels of anxiety symptoms, we did not observe a linear relation between adversity exposure and anxiety across latent profiles. Indeed, individuals in the first latent profile, who had low lifetime adversity exposure and high neural discrimination between threat and safety, displayed levels of anxiety similar to those in the third latent profile (who had high lifetime adversity exposure and showed low neural discrimination between threat and safety). We hypothesize that the first latent profile reflects individuals whose anxiety symptoms may be unrelated to adversity exposure, in turn corresponding to distinct patterns of neural activation during threat and safety learning. These results suggest that although individuals may present similarly clinically (e.g., levels of anxiety that do not statistically differ between profiles 1 and 3), the role of threat and safety learning and its neural and experiential underpinnings may vary substantially across individuals.

The second latent profile (characterized by greater levels of adversity exposure within middle childhood and adolescence relative to the first latent profile, with neural threat/safety discrimination driven by increased prefrontal activation to safety) displayed the lowest levels of anxiety in young adulthood. This finding contrasts with our hypothesis that individuals in the latent profile with the lowest levels of adversity exposure would also display the lowest levels of anxiety symptoms. Instead, results suggest that among some individuals, moderate levels of adversity exposure during middle childhood and adolescence could be associated with processes that, together with a specific neural phenotype, foster future resilience to anxiety. These protective effects may be mediated in part by the prefrontal cortex[22,126]. The prefrontal cortex exhibits a protracted developmental timeline and undergoes circuit refinement throughout adolescence and into early adulthood[50–52,127,128]. Viewed through an adaptive lens[129], enhanced prefrontal neuroplasticity during the adolescent period may facilitate neural adaptations to chronic, mild stress that promote resilience to future stressors[8,126]. Indeed, longitudinal evidence from a large study characterizing neural correlates of a resilience '*r*' factor found that increased reward responsivity in prefrontal regions and decreased hippocampal response to threat were associated with higher '*r*' factor scores[130]. These results dovetail with the present findings to suggest that relatively greater prefrontal engagement and lower subcortical reactivity may reflect more 'resilient' functioning across task domains.

Further, studies in rodents and non-human primates[21,24–26] as well as in humans[131–134] suggest that low-to-moderate levels of stress during development may promote resilience against future stressors. These reports are consistent with the present results, which suggest that both number of exposures and timing of exposures may play a role in shaping neural and behavioral phenotypes. In sensitivity analyses, we demonstrated that the present profile solution cannot be recapitulated using a measure of cumulative adversity exposure instead of adversity exposures binned by developmental stage. Further, there was no evidence of a sample-wide, non-linear association between cumulative adversity exposure and anxiety symptoms. Together, these results suggest that the developmental timing of adversity may meaningfully interact with the number, or frequency, of adversity exposures together with neural functioning to shape behavior and that adversity exposure during middle childhood and adolescence may be particularly impactful. These findings align with results from a recent study, which identified middle childhood as an especially important time when key experiential elements of adversity such as predictability and controllability might buffer against risk for adversity-related psychopathology[70], highlighting the importance of this developmental stage for understanding resilience. While parsing additional experiential elements of adversity was not possible in the current sample, future studies that examine neurobiological processes linking experiential and timing-related elements of adversity with later mental health will be helpful for understanding mechanisms of resilience.

Limitations

The present findings should be interpreted in the context of several important limitations. First, this study was conducted with a laboratory-based sample of participants who completed detailed clinical interviews, resulting in rich phenotyping of adversity exposure. While this type of methodological detail holds promise for advancing the science of adversity exposure and neurodevelopment, it constrains the sample size that is feasible to collect. Although the latent profiles reported in this study demonstrated acceptable entropy and distance, the modest overall sample size may have restricted the ability of LPA to identify and resolve more "rare" profiles that represent relatively small proportions of the overall sample[114,135]. Similarly, due to sample size we did not parse adversity exposure by additional relevant dimensions, such as predictability, controllability, threat, or deprivation[6,9,136]. Future work probing interactions between the developmental timing of adversity and such dimensions could provide more granular insight into how adverse events impact threat and safety learning and mental health. Additionally, adversity exposure was assessed via retrospective report through clinical interviews in the present study. Although concordance between retrospective and prospective report of adversity has been shown to be higher when data are collected through interviews relative to questionnaires[137], participants may not have been able to recall all adverse events, particularly those experienced in early childhood[138]. Despite this limitation[139], retrospective report of adversity has been shown to better predict adult mental health symptoms compared with more "objective" adversity measures[140,141]. Future studies with large-scale longitudinal cohorts that systematically characterize children's environments, including both adversity exposure and putative resilience factors[142,143], are needed to disentangle both the role of childhood experiences in shaping neurodevelopment and mental health, as well as the comparative predictive utility of prospective and retrospective report of adversity exposure[137]. The present study also comprised predominantly high-functioning young adults (i.e., who were able to complete research paradigms including an aversive learning fMRI task and scan) and excluded several comorbid diagnoses, which may partially explain why the second profile (which showed moderate adversity exposure during middle childhood and adolescence, increased neural activation to safety, and lower anxiety in young adulthood) comprised the largest proportion of study participants. While resilience remains a common outcome following adversity[144], how the present findings and interpretations may differ among individuals with severe psychopathology remains to be explored. Finally, our sample comprised young

adults who were predominantly White with higher income and college educations. Replicating these findings in a large, socio-economically and demographically diverse sample will be important for understanding the extent to which these associations generalize to the broader population[145].

Conclusions

The present study employed a data-driven, person-centered approach to characterize shared patterns of adversity exposure across development and neural discrimination between threat and safety in young adulthood. Our findings are consistent with previous research linking high levels of adversity exposure with diminished neural discrimination in responding to threat and safety cues and suggest that low-to-moderate levels of adversity exposure during middle childhood and adolescence may relate to neural threat/safety discrimination in ways that foster resilience to future anxiety for some young adults. Further, our findings suggest that distinct patterns of corticolimbic activation when responding to threat and safety may underlie relations between adversity exposure and anxiety. Ultimately, better understanding of how the developmental timing and number of adversity exposures jointly influence the development of corticolimbic circuits supporting affective learning and mental health could help to elucidate the neural underpinnings of anxiety disorders and inform personalized, developmentally-informed interventions for youth exposed to adversity.

Data availability

The dataset used in this study can be found at https://github.com/Yale-CANDLab/Shapes_DevAdversity_LPA.

Code availability

Analysis code for this study can be found at https://github.com/Yale-CANDLab/Shapes_DevAdversity_LPA.

Received: 29 July 2024; Accepted: 16 January 2025;
Published online: 05 March 2025

References

1. Green, J. G. et al. Childhood adversities and adult psychiatric disorders in the national comorbidity survey replication I: associations with first onset of DSM-IV disorders. *Arch. Gen. Psychiatry* **67**, 113–123 (2010).
2. Teicher, M. H., Andersen, S. L., Polcari, A., Anderson, C. M. & Navalta, C. P. Developmental neurobiology of childhood stress and trauma. *Psychiatr. Clin. N. Am.* **25**, 397–426 (2002). vii-viii.
3. Copeland, W. E. et al. Association of childhood trauma exposure with adult psychiatric disorders and functional outcomes. *JAMA Netw. Open* **1**, e184493 (2018).
4. Bonanno G. A., Chen S., Galatzer-Levy I. R. Resilience to potential trauma and adversity through regulatory flexibility. *Nat. Rev. Psychol*. **2**, 663–675 (2023).
5. Brutzman, B., Bustos, T. E., Hart, M. J. & Neal, J. W. A new wave of context: Introduction to the special issue on socioecological approaches to psychology. *Transl. Issues Psychol. Sci.* **8**, 177–184 (2022).
6. Cohodes, E. M., Kitt, E. R., Baskin-Sommers, A. & Gee, D. G. Influences of early-life stress on frontolimbic circuitry: Harnessing a dimensional approach to elucidate the effects of heterogeneity in stress exposure. *Dev. Psychobiol.* **63**, 153–172 (2021).
7. Ellis, B. J., Figueredo, A. J., Brumbach, B. H. & Schlomer, G. L. Fundamental dimensions of environmental risk: the impact of harsh versus unpredictable environments on the evolution and development of life history strategies. *Hum. Nat. Hawthorn. N.* **20**, 204–268 (2009).
8. Gee, D. G. & Casey, B. The impact of developmental timing for stress and recovery. *Neurobiol. Stress* **1**, 184–194 (2015).
9. McLaughlin, K. A., Sheridan, M. A. & Lambert, H. K. Childhood adversity and neural development: deprivation and threat as distinct dimensions of early experience. *Neurosci. Biobehav Rev.* **47**, 578–591 (2014).
10. Andersen, S. L. Trajectories of brain development: point of vulnerability or window of opportunity? *Neurosci. Biobehav Rev.* **27**, 3–18 (2003).
11. Greenough, W. T., Black, J. E. & Wallace, C. S. Experience and brain development. *Child Dev.* **58**, 539–559 (1987).
12. Tottenham N., Sheridan M. A review of adversity, the amygdala and the hippocampus: a consideration of developmental timing. *Front. Hum. Neurosci*. (2010). https://www.frontiersin.org/articles/10.3389/neuro.09.068.2009
13. Tsoory, M. & Richter-Levin, G. Learning under stress in the adult rat is differentially affected by 'juvenile' or 'adolescent' stress. *Int J. Neuropsychopharmacol.* **9**, 713–728 (2006).
14. Green, M. R., Barnes, B. & McCormick, C. M. Social instability stress in adolescence increases anxiety and reduces social interactions in adulthood in male long–evans rats. *Dev. Psychobiol.* **55**, 849–859 (2013).
15. Meyer, H. C., Gerhard, D. M., Amelio, P. A. & Lee, F. S. Pre-adolescent stress disrupts adult, but not adolescent, safety learning. *Behav. Brain Res.* **400**, 113005 (2021).
16. Negrón-Oyarzo, I., Pérez, M. Á., Terreros, G., Muñoz, P. & Dagnino-Subiabre, A. Effects of chronic stress in adolescence on learned fear, anxiety, and synaptic transmission in the rat prelimbic cortex. *Behav. Brain Res.* **259**, 342–353 (2014).
17. Tsotsokou, G., Nikolakopoulou, M., Kouvelas, E. D. & Mitsacos, A. Neonatal maternal separation affects metabotropic glutamate receptor 5 expression and anxiety-related behavior of adult rats. *Eur. J. Neurosci.* **54**, 4550–4564 (2021).
18. Yohn, N. L. & Blendy, J. A. Adolescent chronic unpredictable stress exposure is a sensitive window for long-term changes in adult behavior in mice. *Neuropsychopharmacology* **42**, 1670–1678 (2017).
19. Manzano-Nieves, G., Gaillard, M., Gallo, M. & Bath, K. G. Early life stress impairs contextual threat expression in female, but not male, mice. *Behav. Neurosci.* **132**, 247–257 (2018).
20. Moaddab, M., Wright, K. M. & McDannald, M. A. Early adolescent adversity alters periaqueductal gray/dorsal raphe threat responding in adult female rats. *Sci. Rep.* **10**, 18035 (2020).
21. Chaby L. E. et al. Repeated stress exposure in mid-adolescence attenuates behavioral, noradrenergic, and epigenetic effects of trauma-like stress in early adult male rats. *Sci. Rep*. **10**, 17935 (2020).
22. Cotella E. M. et al. Adolescent stress confers resilience to traumatic stress later in life: role of the prefrontal cortex. *Biol. Psychiatry Glob. Open Sci*. **3**, 274–282 (2022).
23. Montes-Rodríguez, C. J. et al. Activity-dependent synaptic plasticity in the medial prefrontal cortex of male rats underlies resilience-related behaviors to social adversity. *J. Neurosci. Res.* **102**, e25377 (2024).
24. Parker, K. J., Buckmaster, C. L., Schatzberg, A. F. & Lyons, D. M. Prospective investigation of stress inoculation in young monkeys. *Arch. Gen. Psychiatry* **61**, 933–941 (2004).
25. Ricon, T., Toth, E., Leshem, M., Braun, K. & Richter-Levin, G. Unpredictable chronic stress in juvenile or adult rats has opposite effects, respectively, promoting and impairing resilience. *Stress* **15**, 11–20 (2012).
26. Suo, L. et al. Predictable chronic mild stress in adolescence increases resilience in adulthood. *Neuropsychopharmacology* **38**, 1387–1400 (2013).
27. Grasser, L. R. & Jovanovic, T. Safety learning during development: Implications for development of psychopathology. *Behav. Brain Res.* **408**, 113297 (2021).
28. Ruge J. et al. How adverse childhood experiences get under the skin: a systematic review, integration and methodological discussion on threat and reward learning mechanisms. Gillan C. M., Wassum K. M., eds. *eLife*. **13**, e92700 (2024).

29. Qiu, Y., Dou, H., Dai, Y., Li, H. & Lei, Y. The influence of being left behind on fear acquisition and academic performance—a study of left-behind children. *Curr. Psychol.* **42**, 28095–28106 (2022).
30. DeCross, S. N., Sambrook, K. A., Sheridan, M. A., Tottenham, N. & McLaughlin, K. A. Dynamic alterations in neural networks supporting aversive learning in children exposed to trauma: neural mechanisms underlying psychopathology. *Biol. Psychiatry* **91**, 667–675 (2022).
31. Klingelhöfer-Jens M. et al. Reduced discrimination between signals of danger and safety but not overgeneralization is linked to exposure to childhood adversity in healthy adults. *eLife*. **12**, 1–38 (2024).
32. McLaughlin, K. A. et al. Maltreatment exposure, brain structure, and fear conditioning in children and adolescents. *Neuropsychopharmacol. Publ. Am. Coll. Neuropsychopharmacol.* **41**, 1956–1964 (2016).
33. Machlin L., Miller A. B., Snyder J., McLaughlin K. A., Sheridan M. A. Differential associations of deprivation and threat with cognitive control and fear conditioning in early childhood. *Front. Behav. Neurosci*. **13**, 1–14 (2019).
34. Stout, D. M. et al. Dissociable impact of childhood trauma and deployment trauma on affective modulation of startle. *Neurobiol. Stress* **15**, 100362 (2021).
35. Herringa, R. J. et al. Enhanced prefrontal-amygdala connectivity following childhood adversity as a protective mechanism against internalizing in adolescence. *Biol. Psychiatry Cogn. Neurosci. Neuroimaging* **1**, 326–334 (2016).
36. Tottenham, N. et al. Elevated amygdala response to faces following early deprivation. *Dev. Sci.* **14**, 190–204 (2011).
37. van Harmelen, A. L. et al. Enhanced amygdala reactivity to emotional faces in adults reporting childhood emotional maltreatment. *Soc. Cogn. Affect Neurosci.* **8**, 362–369 (2013).
38. Huskey, A., Taylor, D. J. & Friedman, B. H. "Generalized unsafety" as fear inhibition to safety signals in adults with and without childhood trauma. *Dev. Psychobiol.* **64**, e22242 (2022).
39. Wolitzky-Taylor, K. et al. Adversity in early and midadolescence is associated with elevated startle responses to safety cues in late adolescence. *Clin. Psychol. Sci.* **2**, 202–213 (2014).
40. Sicorello, M., Thome, J., Herzog, J. & Schmahl, C. Differential effects of early adversity and posttraumatic stress disorder on amygdala reactivity: the role of developmental timing. *Biol. Psychiatry Cogn. Neurosci. Neuroimaging* **6**, 1044–1051 (2021).
41. Zhu, J., Anderson, C. M., Ohashi, K., Khan, A. & Teicher, M. H. Potential sensitive period effects of maltreatment on amygdala, hippocampal and cortical response to threat. *Mol. Psychiatry* **28**, 5128–5139 (2023).
42. Levy, I. & Schiller, D. Neural computations of threat. *Trends Cogn. Sci.* **25**, 151–171 (2021).
43. Zugman, A., Winkler, A. M. & Pine, D. S. Recent advances in understanding neural correlates of anxiety disorders in children and adolescents. *Curr. Opin. Psychiatry* **34**, 617–623 (2021).
44. Peng, Y. et al. Threat neurocircuitry predicts the development of anxiety and depression symptoms in a longitudinal study. *Biol. Psychiatry Cogn. Neurosci. Neuroimaging* **8**, 102–110 (2023).
45. Sequeira, S. L. et al. Pathways to adolescent social anxiety: testing interactions between neural social reward function and perceived social threat in daily life. *Dev. Psychopathol.* **27**, 1–16 (2024).
46. Borchers, L. R., Gifuni, A. J., Ho, T. C., Kirshenbaum, J. S. & Gotlib, I. H. Threat- and reward-related brain circuitry, perceived stress, and anxiety in adolescents during the COVID-19 pandemic: a longitudinal investigation. *Soc. Cogn. Affect Neurosci.* **19**, nsae040 (2024).
47. Lonsdorf, T. B., Haaker, J. & Kalisch, R. Long-term expression of human contextual fear and extinction memories involves amygdala, hippocampus and ventromedial prefrontal cortex: a reinstatement study in two independent samples. *Soc. Cogn. Affect Neurosci.* **9**, 1973–1983 (2014).
48. Casey, B. J. Beyond simple models of self-control to circuit-based accounts of adolescent behavior. *Annu. Rev. Psychol.* **66**, 295–319 (2015).
49. Alex, A. M. et al. A global multicohort study to map subcortical brain development and cognition in infancy and early childhood. *Nat. Neurosci.* **27**, 176–186 (2024).
50. Larsen, B. & Luna, B. Adolescence as a neurobiological critical period for the development of higher-order cognition. *Neurosci. Biobehav. Rev.* **94**, 179–195 (2018).
51. Sydnor, V. J. et al. Neurodevelopment of the association cortices: patterns, mechanisms, and implications for psychopathology. *Neuron* **109**, 2820–2846 (2021).
52. Sydnor, V. J. et al. Intrinsic activity development unfolds along a sensorimotor–association cortical axis in youth. *Nat. Neurosci.* **26**, 638–649 (2023).
53. Larsen, B. et al. A developmental reduction of the excitation:inhibition ratio in association cortex during adolescence. *Sci. Adv.* **8**, eabj8750 (2022).
54. Olson, I., Von Der Heide, R. J., Alm, K. & Vyas, G. Development of the uncinate fasciculus: implications for theory and developmental disorders. *Dev. Cogn. Neurosci.* **14**, 50–61 (2015).
55. Sisk, L. M. & Gee, D. G. Stress and adolescence: vulnerability and opportunity during a sensitive window of development. *Curr. Opin. Psychol.* **44**, 286–292 (2022).
56. Tottenham, N. Early adversity and the neotenous human brain. *Biol. Psychiatry* **87**, 350–358 (2020).
57. Jovanovic, T. et al. Development of fear acquisition and extinction in children: effects of age and anxiety. *Neurobiol. Learn Mem.* **113**, 135–142 (2014).
58. Michalska, K. J. et al. A developmental analysis of threat/safety learning and extinction recall during middle childhood. *J. Exp. Child Psychol.* **146**, 95–105 (2016).
59. Pattwell, S. S. et al. Altered fear learning across development in both mouse and human. *Proc. Natl Acad. Sci.* **109**, 16318–16323 (2012).
60. Conley, M. I., Hernandez, J., Salvati, J. M., Gee, D. G. & Baskin-Sommers, A. The role of perceived threats on mental health, social, and neurocognitive youth outcomes: a multicontextual, person-centered approach. *Dev. Psychopathol.* **2**, 1–22 (2022).
61. Ricard, J. R., Hyde, L. W. & Baskin-Sommers, A. Person-centered combinations of individual, familial, neighborhood, and structural risk factors differentially relate to antisocial behavior and psychopathology. *Crim. Justice Behav.* **20**, 00938548241246146 (2024).
62. Ruiz, S. G., Brazil, I. A. & Baskin-Sommers, A. Distinct neurocognitive fingerprints reflect differential associations with risky and impulsive behavior in a neurotypical sample. *Sci. Rep.* **13**, 11782 (2023).
63. Magnusson D., Stattin H. Person-context interaction theories. in *Handbook of Child Psychology: Theoretical Models of Human Development* 5th edn, Vol. 1 (John Wiley & Sons, Inc., 1998) 685–759.
64. Vermunt, J. K. Latent class modeling with covariates: two improved three-step approaches. *Polit. Anal.* **18**, 450–469 (2010).
65. Vermunt, J. K. & Magidson, J. Latent class analysis. *Sage Encycl. Soc. Sci. Res Methods* **2**, 549–553 (2004).
66. McLaughlin, K. A. et al. Childhood adversities and adult psychiatric disorders in the national comorbidity survey replication II: associations with persistence of DSM-IV disorders. *Arch. Gen. Psychiatry* **67**, 124–132 (2010).
67. Cohodes, E. M. et al. Development and validation of the Dimensional Inventory of Stress and Trauma Across the Lifespan (DISTAL): a novel assessment tool to facilitate the dimensional study of psychobiological sequelae of exposure to adversity. *Dev. Psychobiol.* **65**, e22372 (2023).
68. Patridge, E. F. & Bardyn, T. P. Research Electronic Data Capture (REDCap). *J. Med Libr Assoc. JMLA* **106**, 142–144 (2018).

69. Steinberg A. M., Brymer M. J., Decker K. B., Pynoos R. S., Address M. The University of California at Los Angeles post-traumatic stress disorder reaction index. https://link.springer.com/content/pdf/10.1007%2Fs11920-004-0048-2.pdf
70. Cohodes, E. M. et al. Characterizing experiential elements of early-life stress to inform resilience: Buffering effects of controllability and predictability and the importance of their timing. *Dev. Psychopathol.* **27**, 1–14 (2023).
71. Angulo, M. et al. Psychometrics of the Screen for Adult Anxiety Related Disorders (SCAARED)- a new scale for the assessment of DSM-5 anxiety disorders. *Psychiatry Res.* **253**, 84–90 (2017).
72. Elliott, D. M. & Briere, J. Sexual abuse trauma among professional women: validating the Trauma Symptom Checklist-40 (TSC-40). *Child Abus. Negl.* **16**, 391–398 (1992).
73. Rescorla L. A., Achenbach T. M. The Achenbach System of Empirically Based Assessment (ASEBA) for ages 18 to 90 years. in *The Use of Psychological Testing for Treatment Planning and Outcomes Assessment: Instruments for Adults* 3rd edn, Vol. 3 (Lawrence Erlbaum Associates Publishers, 2004) 115–152.
74. Casey, B. J. et al. The Adolescent Brain Cognitive Development (ABCD) study: imaging acquisition across 21 sites. *Dev. Cogn. Neurosci.* **32**, 43–54 (2018).
75. Glasser, M. F. et al. Consortium. The minimal preprocessing pipelines for the Human Connectome Project. *NeuroImage* **80**, 105–124 (2013).
76. Kribakaran, S. et al. Neural circuitry involved in conditioned inhibition via safety signal learning is sensitive to trauma exposure. *Neurobiol. Stress.* **17**, 100497 (2022).
77. Meyer H. C. et al. Ventral hippocampus interacts with prelimbic cortex during inhibition of threat response via learned safety in both mice and humans. *Proc Natl Acad Sci*. **116**, 26970–26979 (2019).
78. Odriozola P. et al. Hippocampal involvement in safety signal learning varies with anxiety among healthy adults. *Biol Psychiatry Glob. Open Sci*. S2667174323000769 (2023).
79. Neumann, D. L., Waters, A. M. & Westbury, H. R. The use of an unpleasant sound as the unconditional stimulus in aversive Pavlovian conditioning experiments that involve children and adolescent participants. *Behav. Res Methods* **40**, 622–625 (2008).
80. Lonsdorf, T. B. et al. Don't fear 'fear conditioning': methodological considerations for the design and analysis of studies on human fear acquisition, extinction, and return of fear. *Neurosci. Biobehav Rev.* **77**, 247–285 (2017).
81. Gorgolewski, K. J. et al. The brain imaging data structure, a format for organizing and describing outputs of neuroimaging experiments. *Sci. Data* **3**, 160044 (2016).
82. Chang, H. & Fitzpatrick, J. M. A technique for accurate magnetic resonance imaging in the presence of field inhomogeneities. *IEEE Trans. Med Imaging* **11**, 319–329 (1992).
83. Hagler, D. J. et al. Image processing and analysis methods for the Adolescent Brain Cognitive Development Study. *NeuroImage* **202**, 116091 (2019).
84. Morgan, P. S., Bowtell, R. W., McIntyre, D. J. O. & Worthington, B. S. Correction of spatial distortion in EPI due to inhomogeneous static magnetic fields using the reversed gradient method. *J. Magn. Reson, Imaging JMRI* **19**, 499–507 (2004).
85. Jenkinson, M., Bannister, P., Brady, M. & Smith, S. Improved optimization for the robust and accurate linear registration and motion correction of brain images. *NeuroImage* **17**, 825–841 (2002).
86. Tukey, J. W. *Exploratory Data Analysis*, Vol 2 (Addison-Wesley, 1977).
87. Power, J. D., Barnes, K. A., Snyder, A. Z., Schlaggar, B. L. & Petersen, S. E. Spurious but systematic correlations in functional connectivity MRI networks arise from subject motion. *NeuroImage* **59**, 2142–2154 (2012).
88. Jenkinson, M., Beckmann, C. F., Behrens, T. E. J., Woolrich, M. W. & Smith, S. M. Fsl *NeuroImage* **62**, 782–790 (2012).
89. Kredlow, A. M., Fenster, R. J., Laurent, E. S., Ressler, K. J. & Phelps, E. A. Prefrontal cortex, amygdala, and threat processing: implications for PTSD. *Neuropsychopharmacology* **47**, 247–259 (2022).
90. Milad, M. R. & Quirk, G. J. Fear extinction as a model for translational neuroscience: ten years of progress. *Annu Rev. Psychol.* **63**, 129–151 (2012).
91. Odriozola, P. & Gee, D. G. Learning about safety: conditioned inhibition as a novel approach to fear reduction targeting the developing brain. *Am. J. Psychiatry* **178**, 136–155 (2021).
92. Horien, C., Shen, X., Scheinost, D. & Constable, R. T. The individual functional connectome is unique and stable over months to years. *NeuroImage* **189**, 676–687 (2019).
93. Mackey, S. & Petrides, M. Architecture and morphology of the human ventromedial prefrontal cortex. *Eur. J. Neurosci.* **40**, 2777–2796 (2014).
94. Rolls, E. T., Huang, C. C., Lin, C. P., Feng, J. & Joliot, M. Automated anatomical labelling atlas 3. *NeuroImage* **206**, 116189 (2020).
95. Van Dijk, K. R. A., Sabuncu, M. R. & Buckner, R. L. The influence of head motion on intrinsic functional connectivity MRI. *NeuroImage* **59**, 431–438 (2012).
96. Rapuano K. M. et al. Behavioral and brain signatures of substance use vulnerability in childhood. *Dev. Cogn. Neurosci*. **46**, 100878 (2020).
97. Sisk, L. M. et al. Genetic variation in endocannabinoid signaling is associated with differential network-level functional connectivity in youth. *J. Neurosci. Res* **100**, 731–743 (2022).
98. Seabold, S. & Perktold, J. Statsmodels: econometric and modeling with Python. In *Proc 9th Python in Science Conference, Austin, 28 June-3 July*. 57–61. https://doi.org/10.25080/Majora-92bf1922-011 (2010).
99. Eliot, L., Ahmed, A., Khan, H. & Patel, J. Dump the "dimorphism": Comprehensive synthesis of human brain studies reveals few male-female differences beyond size. *Neurosci. Biobehav Rev.* **125**, 667–697 (2021).
100. Akinwande, M. O., Dikko, H. G. & Samson, A. Variance inflation factor: as a condition for the inclusion of suppressor variable(s) in regression analysis. *Open J. Stat.* **05**, 754–767 (2015).
101. van Rossum G. Python tutorial. in *Technical Report CS-R9526* (Centrum voor Wiskunde en Informatica (CWI), Amsterdam, 1995).
102. R Core Team. R: A language and environment for statistical computing. Published online 2019. https://www.R-project.org/
103. Morin S. et al. StepMix: a python package for pseudo-likelihood estimation of generalized mixture models with external variables. http://arxiv.org/abs/2304.03853
104. Dalmaijer, E. S., Nord, C. L. & Astle, D. E. Statistical power for cluster analysis. *BMC Bioinform.* **23**, 205 (2022).
105. Bolck, A., Croon, M. & Hagenaars, J. Estimating latent structure models with categorical variables: one-step versus three-step estimators. *Polit. Anal.* **12**, 3–27 (2004).
106. Schwarz, G. Estimating the dimension of a model. *Ann. Stat.* **6**, 461–464 (1978).
107. Akaike H. Akaike's information criterion. in Lovric M. (ed) *International Encyclopedia of Statistical Science* (Springer, 2011).
108. Celeux, G. & Soromenho, G. An entropy criterion for assessing the number of clusters in a mixture model. *J. Classif.* **13**, 195–212 (1996).
109. McLachlan, G. J., Lee, S. X. & Rathnayake, S. I. Finite mixture models. *Annu Rev. Stat. Appl.* **6**, 355–378 (2019).
110. Mann, H. B. & Whitney, D. R. On a test of whether one of two random variables is stochastically larger than the other. *Ann. Math. Stat.* **18**, 50–60 (1947).

111. Benjamini, Y. & Hochberg, Y. Controlling the False Discovery Rate: A Practical and Powerful Approach to Multiple Testing. *J. R. Stat. Soc. Ser. B Methodol.* **57**, 289–300 (1995).
112. Games, P. A. & Howell, J. F. Pairwise multiple comparison procedures with unequal N's and/or variances: a Monte Carlo study. *J. Educ. Stat.* **13**, 113–125 (1976).
113. Vallat, R. Pingouin: statistics in Python. *J. Open Source Softw.* **3**, 1026 (2018).
114. Nylund-Gibson, K. & Choi, A. Y. Ten frequently asked questions about latent class analysis. *Transl. Issues Psychol. Sci.* **4**, 440–461 (2018).
115. Tein, J. Y., Coxe, S. & Cham, H. Statistical power to detect the correct number of classes in latent profile analysis. *Struct. Equ. Model Multidiscip. J.* **20**, 640–657 (2013).
116. Jarque, C. M. & Bera, A. K. A test for normality of observations and regression residuals. *Int. Stat. Rev. Rev. Int. Stat.* **55**, 163 (1987).
117. Solmi, M. et al. Age at onset of mental disorders worldwide: large-scale meta-analysis of 192 epidemiological studies. *Mol. Psychiatry* **27**, 281–295 (2022).
118. Bath, K. G. Synthesizing views to understand sex differences in response to early life adversity. *Trends Neurosci.* **43**, 300–310 (2020).
119. Kessler, R. C. et al. Lifetime prevalence and age-of-onset distributions of DSM-IV disorders in the National Comorbidity Survey Replication. *Arch. Gen. Psychiatry* **62**, 593–602 (2005).
120. Rakesh, D. & Whittle, S. Socioeconomic status and the developing brain – A systematic review of neuroimaging findings in youth. *Neurosci. Biobehav Rev.* **130**, 379–407 (2021).
121. Tooley U. A. et al. Associations between neighborhood SES and functional brain network development. *Cereb. Cortex* **30**, 1–19 (2019).
122. Walker, J. A. Chapter 16 ANOVA tables. In *Elements of Statistical Modeling for Experimental Biology*. https://www.middleprofessor.com/files/applied-biostatistics_bookdown/_book/anova-tables (2018).
123. Fox J., Weisberg S. *An R Companion to Applied Regression*. Third. (Sage, 2019). https://www.john-fox.ca/Companion/
124. Kassambara A. rstatix: pipe-friendly framework for basic statistical tests (2023). https://cran.r-project.org/web/packages/rstatix/index.html
125. Nylund, K. L., Asparouhov, T. & Muthén, B. O. Deciding on the number of classes in latent class analysis and growth mixture modeling: a Monte Carlo simulation study. *Struct. Equ. Model Multidiscip. J.* **14**, 535–569 (2007).
126. Maier, S. F. & Watkins, L. R. Role of the medial prefrontal cortex in coping and resilience. *Brain Res.* **1355**, 52–60 (2010).
127. Giedd, J. N. et al. Brain development during childhood and adolescence: a longitudinal MRI study. *Nat. Neurosci.* **2**, 861–863 (1999).
128. Gogtay N. et al. Dynamic mapping of human cortical development during childhood through early adulthood. *Proc. Natl Acad. Sci.* **101**, 8174–8179 (2004).
129. Ellis, B. J., Bianchi, J., Griskevicius, V. & Frankenhuis, W. E. Beyond risk and protective factors: an adaptation-based approach to resilience. *Perspect. Psychol. Sci.* **12**, 561–587 (2017).
130. Van Rooij S. J. H., et al. Defining the r factor for post-trauma resilience and its neural predictors. *Nat. Ment. Health* **2**, 680–693 (2024).
131. Oshri, A., Cui, Z., Carvalho, C. & Liu, S. Is perceived stress linked to enhanced cognitive functioning and reduced risk for psychopathology? Testing the hormesis hypothesis. *Psychiatry Res.* **314**, 114644 (2022).
132. Oshri A. et al. Strengthening through adversity: the hormesis model in developmental psychopathology. *Dev. Psychopathol*. **36**, 2390–2406 (2024).
133. Seery, M. D. Resilience: a silver lining to experiencing adverse life events? *Curr. Dir. Psychol. Sci.* **20**, 390–394 (2011).
134. Seery, M. D., Leo, R. J., Lupien, S. P., Kondrak, C. L. & Almonte, J. L. An upside to adversity?: Moderate cumulative lifetime adversity is associated with resilient responses in the face of controlled stressors. *Psychol. Sci.* **24**, 1181–1189 (2013).
135. Dalmaijer E. S. Tutorial: a priori estimation of sample size, effect size, and statistical power for cluster analysis, latent class analysis, and multivariate mixture models. Preprint at https://arxiv.org/abs/2309.00866 (2023).
136. Ellis, B. J., Sheridan, M. A., Belsky, J. & McLaughlin, K. A. Why and how does early adversity influence development? Toward an integrated model of dimensions of environmental experience. *Dev. Psychopathol.* **14**, 1–25 (2022).
137. Baldwin, J. R., Reuben, A., Newbury, J. B. & Danese, A. Agreement between prospective and retrospective measures of childhood maltreatment: a systematic review and meta-analysis. *JAMA Psychiatry* **76**, 584–593 (2019).
138. Williams, L. M. Recall of childhood trauma: a prospective study of women's memories of child sexual abuse. *J. Consult Clin. Psychol.* **62**, 1167–1176 (1994).
139. Brewin, C. R., Andrews, B. & Gotlib, I. H. Psychopathology and early experience: a reappraisal of retrospective reports. *Psychol. Bull.* **113**, 82–98 (1993).
140. Baldwin J. R., Coleman O., Francis E. R., Danese A. Prospective and retrospective measures of child maltreatment and their association with psychopathology: a systematic review and meta-analysis. *JAMA Psychiatry* **81**, 769-781 (2024).
141. Francis, E. R., Tsaligopoulou, A., Stock, S. E., Pingault, J. B. & Baldwin, J. R. Subjective and objective experiences of childhood adversity: a meta-analysis of their agreement and relationships with psychopathology. *J. Child Psychol. Psychiatry* **64**, 1185–1199 (2023).
142. Fritz J., de Graaff A. M., Caisley H., van Harmelen A. L., Wilkinson P. O. A systematic review of amenable resilience factors that moderate and/or mediate the relationship between childhood adversity and mental health in young people. *Front. Psychiatry* **9**, 1–17 (2018).
143. Van Harmelen, A. L. et al. Adolescent friendships predict later resilient functioning across psychosocial domains in a healthy community cohort. *Psychol. Med.* **47**, 2312–2322 (2017).
144. Bonanno, G. A. & Westphal, M. The three axioms of resilience. *J. Trauma Stress*. **37**, 717–723 (2024).
145. Gurven, M. D. Broadening horizons: sample diversity and socioecological theory are essential to the future of psychological science. *Proc. Natl Acad. Sci.* **115**, 11420–11427 (2018).

Acknowledgements

This research was supported by funding from National Institutes of Health (NIH) Director's Early Independence Award (DP5OD021370), Brain & Behavior Research Foundation (NARSAD) Young Investigator Award, National Science Foundation (NSF) CAREER Award (BCS-2145372), Jacobs Foundation Early Career Research Fellowship, and The Society for Clinical Child and Adolescent Psychology (Division 53 of the American Psychological Association) Richard "Dick" Abidin Early Career Award and Grant to DGG; Yale University Wu Tsai Institute (WTI) Innovation Grant to ABS; NSF Graduate Research Fellowship Program award (NSF DGE-1752134) and a Dissertation Funding Award from the Society for Research in Child Development to LMS; Yale Child Study Center Postdoctoral T32MH18268 and Brain & Behavior Research Foundation (NARSAD) Young Investigator Award #28436 to TJK; NSF Graduate Research Fellowship Program award (NSF DGE-1752134) and a Scholar Award granted by the International Chapter of the Philanthropic Educational Organization (P.E.O. Foundation) to PO; NIMH National Research Service Award (NRSA F30MH124271) to S.K.; NSF Graduate Research Fellowship Program award (NSF DGE-1752134), American Psychological Foundation Elizabeth

Munsterberg Koppitz Child Psychology Graduate Fellowship, The Society for Clinical Child and Adolescent Psychology (Division 53 of the American Psychological Association) Donald Routh Dissertation Grant, a Dissertation Funding Award from the Society for Research in Child Development, a Dissertation Research Award from the American Psychological Association, an American Dissertation Fellowship from the American Association of University Women (AAUW), and a Scholar Award granted by the International Chapter of the Philanthropic Educational Organization (P.E.O. Foundation) to EMC; a Scholar Award granted by the International Chapter of the Philanthropic Educational Organization (P.E.O. Foundation), UMN Doctoral Dissertation Fellowship, and Norman and Edith Garmezy Fellowship to HRH; and Janet and Sheldon (1959) Razin Fellowship (MIT) to SJZ. The funders had no role in study design, data collection and analysis, decision to publish, or preparation of the manuscript. We are grateful to each of the participants, without whom this study would not have been possible. We thank Elizabeth Kitt for overseeing quality assessment for a portion of the skin conductance response data included in this study and Jeffrey Mandell for contributions to the processing pipeline; Zhiliang Fang, Emma Goodman, Cristian Hernandez, Zoe Hopson, Neida Moreno, Cristina Nardini, Luise Pruessner, Sophie Rader, Beatriz Rios, Hannah Spencer, and Janeen Thomas for their assistance with data collection; and Reta Behnam, Bahar Bouzarjomehri, Rob Colgate, Alice Dyer, Nathalie Eid, Gillian Gold, Emma Goodman, Ana Greenberg, Cristian Hernandez, Jenn Huo, Amy Kwarteng, Brandon Lopez, Lindiwe Mayinja, Olivia Meisner, Lauren Quintela, Isabel Santiuste, Nisan Sele, Georgia Spurrier, Ashley Talton, Alissa Wong, and Daphne Zhu for their assistance with quality assessment of data used in this study. We would also like to thank Dr. Edwin Dalmaijer for his assistance with conceptualizing the power analyses for LPA modeling.

Author contributions

D.G.G., L.M.S., E.M.C., and P.O. contributed to study design. L.M.S., A.B.S., and D.G.G. conceptualized and designed the analyses for this project. T.J.K. and S.R. provided feedback on project and analytic design. L.M.S. analyzed the data and interpreted the findings with support from A.B.S. and D.G.G. T.J.K. reviewed code and analyses. E.M.C., S.M., J.C.P., P.O., S.K., J.T.H., S.J.Z., H.R.H., C.C., and L.M.S. contributed to data collection. L.M.S., P.O., E.M.C., S.M., J.C.P., and H.R.H. contributed to quality assessment and data validation. L.M.S. drafted the paper and T.J.K., S.R., P.O., S.K., E.M.C., H.R.H., A.B.S., and D.G.G. provided review and editing.

Competing interests

The authors declare no competing interests.

Additional information

Supplementary information The online version contains supplementary material available at https://doi.org/10.1038/s44271-025-00193-x.

Correspondence and requests for materials should be addressed to Lucinda M. Sisk or Dylan G. Gee.

Peer review information *Communications Psychology* thanks Mattia Gerin, M. Justin Kim and Jessica Buthmann for their contribution to the peer review of this work. Primary Handling Editor: Jennifer Bellingtier. A peer review file is available.